Acta Crystallographica Section C
Crystal Structure Communications
ISSN 0108-2701

2,2′-(Ethane-1,2-diyl)bis[2-(5-bromothiophen-2-yl)-1,3-dioxolane] at 100 K refined using a multipolar atom model

Maqsood Ahmed,[a] Sajida Noureen,[b] Philippe C. Gros,[b] Benoit Guillot[a] and Christian Jelsch[a]*

[a]CNRS UMR 7036 (CRM^2), Laboratoire de Cristallographie, Résonance Magnétique et Modélisations, Faculté des Sciences et Techniques–UHP, BP-239, 54506 Vandoeuvre-lès-Nancy Cedex, France, and [b]UMR CNRS 7565 (SOR), Synthèse Organométallique et Réactivité, Faculté des Sciences et Techniques–UHP, BP-239, 54506 Vandoeuvre-lès-Nancy Cedex, France
Correspondence e-mail: christian.jelsch@crm2.uhp-nancy.fr

Received 12 April 2011
Accepted 7 July 2011
Online 28 July 2011

The title compound, $C_{16}H_{16}Br_2O_4S_2$, which is a precursor for the synthesis of oligothiophenes and their substituted homologues, was synthesized and its X-ray crystal structure determined at 100 K. The experimental electron-density parameters for the available atom types were transferred from the ELMAM2 database. The compound lies about an inversion centre, which coincides with the mid-point of a C—C bond. The molecules in the crystal are linked by several types of weak interactions; the largest contact surfaces are for H···H and H···Br.

Comment

In the recent past, oligothiophenes and their substituted homologues have attracted the attention of the scientific community as they are a promising class of organic semiconductor materials for applications in the production of organic field-effect transistors and as electronic devices (Roncali, 1992). These π-conjugated materials have found important applications, for example in organic solar cells (Ma *et al.*, 2008; Gao *et al.*, 2008; Cao *et al.*, 2009; Rousseau *et al.*, 2010) and OLEDs (organic light-emitting diodes) (Mazzeo *et al.*, 2003; Li *et al.*, 2005). Compared to non-organic semiconductors, they offer many advantages such as the fact that their electronic properties, notably the band gap, are tuneable by chemical modification. The title compound, (I), has been used as a precursor for these materials (Kreyes, Amirkhani *et al.*, 2010; Kreyes, Ellinger *et al.*, 2010). The reactive C—Br bonds allow for further functionalizations and polymer chain extension. Therefore, a detailed knowledge of the structural parameters, stereochemistry, planarity and the mutual arrangement of the molecule is required to understand better the structure–property relationships. In addition, knowledge of the intra- and intermolecular interactions is crucial to rationally carry out chemical substitutions. The structure of (I) was briefly reported previously at 223 (2) K by Ellinger *et al.* (2007). The structure has been redetermined at low temperature (100 K), refined using a multipolar atom model and is described here in greater detail.

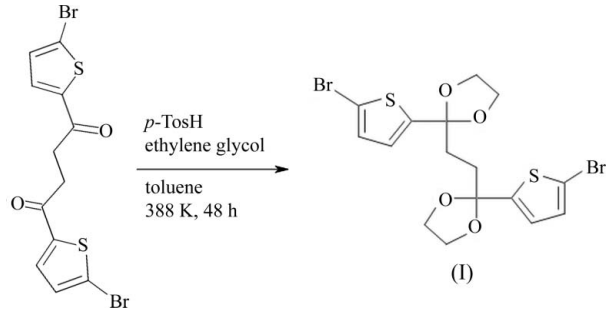

(I)

The commonly used spherical atom approximation (IAM, Independent Atom Model) does not give all the information about the intermolecular interactions and is likely to produce severe systematic errors in the refined atomic parameters (Ruysink & Vos, 1974). Experimental electron-density analysis is carried out by X-ray diffraction of mono-crystals at ultra high resolution ($d_{min} \simeq 0.5$ Å; Coppens, 1998). A difficulty in crystallography is the separation of the anisotropic atomic mean-square displacements from the static molecular electron distribution (Hirshfeld, 1976). Proper experimental deconvolution requires diffraction data measured at ultra high resolution. However, effective thermal displacement deconvolution and meaningful electron-density distributions can be achieved even at lower resolutions by transferring the parameters from an electron-density database (Pichon-Pesme *et al.*, 1995; Jelsch *et al.*, 1998; Dittrich *et al.*, 2004, 2005, 2007). Transferring electron-density parameters is comparable to constraining the deformation parameters at their most likely values. The transferability of atomic electron densities was tested for the first time by Brock *et al.* (1991) who applied atomic charge-density parameters from an accurate low-temperature study of perylene to diffraction data collected at several temperatures on naphthalene and anthracene crystals.

The ELMAM database (Zarychta *et al.*, 2007) has been extended to ELMAM2 (Domagała *et al.*, 2011) from protein atom types to common organic molecules and is based on optimal local coordinate systems (Domagała & Jelsch, 2008). An automatic transfer procedure of the ELMAM2 database is now available in the *MoPro* software (Guillot *et al.*, 2001; Jelsch *et al.*, 2005). The different atom types in a molecule are recognized according to the nature and number of their neighbours. For most atoms, only the first shell of neighbours is analysed, while for H and O atoms, the second and third shells are investigated, respectively (Domagała & Jelsch, 2008; Domagała *et al.*, 2011).

Using the transferability principle, a multipolar model is applied for the molecule (I) and only the structural parameters (scale factor, atomic coordinates and displacement parameters) are refined. The Fourier residual maps are improved, notably on the covalent bonds due to the proper electron- density modelling. The r.m.s. residual density is

 doi:10.1107/S0108270111027247

reduced from 0.090 (IAM) to 0.075 e Å^{-3} in the transferred model. In addition to the detailed structural description, the redetermined structure also has significantly better refinement statistics than the previous one. Using an $I/\sigma(I) > 2$ cutoff, the crystallographic $wR_2(F)$ factors are indeed 4.1 and 2.7% for the IAM and the transferred–multipolar structures, respectively.

There is one half of the molecule in the asymmetric unit and four molecules in the unit cell. The two symmetry-equivalent half molecules are linked by an inversion centre in the middle of the C8—C8^{i} bond (Fig. 1).

The molecular assembly is built from five different types of interactions. Dimers of molecules, related by an inversion centre, are formed by two very weak C8—H8*B*···O2 hydrogen bonds (Table 1). There is a short S1···H3 contact of 2.985 Å in a dimer of molecules related by *b*-axis translation.

Two different neighbouring molecules are in van der Waals interaction with the Br atom. The Br atom makes a contact with O1 of the dioxolane ring of an adjacent molecule at a distance of 3.160 (1) Å, which is shorter than the sum of the two van der Waals radii (3.37 Å). An even shorter Br···O contact of 3.0 Å occurs in the structure of protein human aldose reductase complexed with an inhibitor (Muzet *et al.*, 2003). The C1—Br1···O1 angle of 168.7 (1)° (Fig. 2) is almost linear and is consistent with the value found in the review by Auffinger *et al.* (2004) of halogen–oxygen short interactions in biomolecules. Nyburg & Faerman (1985) revised the van der Waals radii for several atoms bonded to C atoms in molecular crystals; the proposed radius for bromine is 1.84 Å in the equatorial directions and 1.54 Å in the polar direction opposite to the C—Br bond. The direction-dependent effective van der Waals radius is related to the anisotropic electron density of the Br atom. Bromine and more generally halogen atoms (such as I, Cl or F) show a torus of electron accumulation in the equatorial region, while the polar region is electron depleted (Fig. 3). Halogen atoms *X* can therefore form elec-

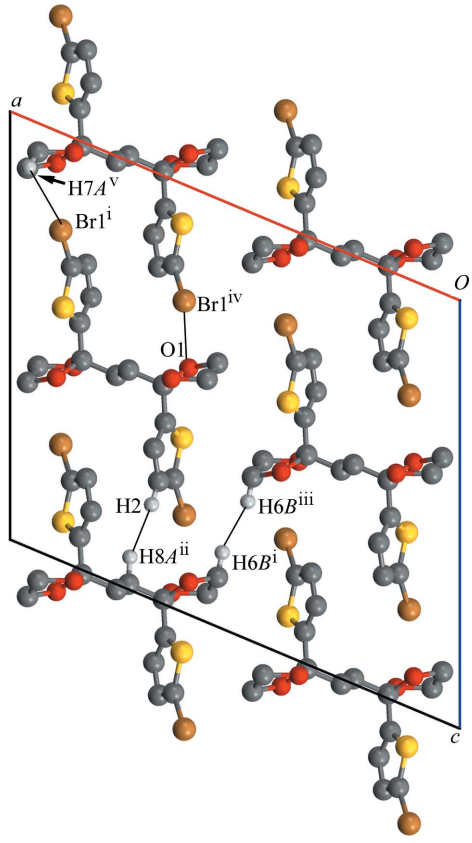

Figure 2
The crystal packing of (I), viewed along the *b* axis, showing different intermolecular interactions (thin lines). [Symmetry codes: (i) $-x+\frac{3}{2}, -y+\frac{1}{2}, -z+1$; (ii) $x, -y, z+\frac{1}{2}$; (iii) $-x+1, -y, -z+1$; (iv) $x, -y+1, z-\frac{1}{2}$; (v) $-x+\frac{3}{2}, y+\frac{1}{2}, -z+\frac{1}{2}$.]

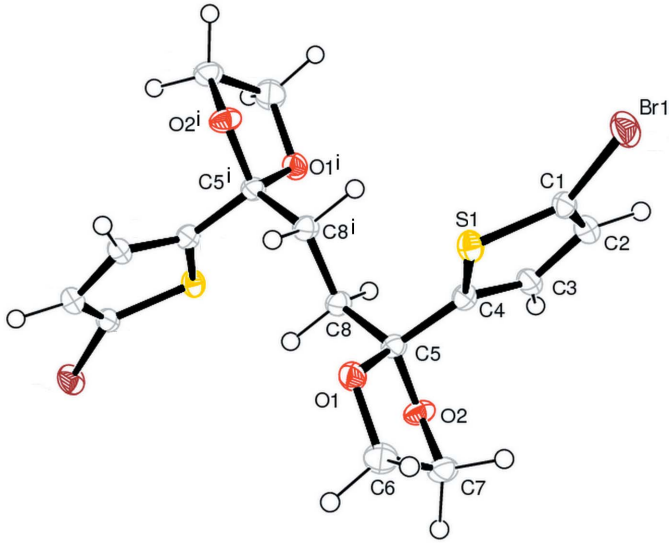

Figure 1
The molecular configuration and atom-numbering scheme for the title compound. Displacement ellipsoids are drawn at the 50% probability level and H atoms are not labelled. [Symmetry code: (i) $-x+\frac{3}{2}, -y+\frac{1}{2}, -y+1$.]

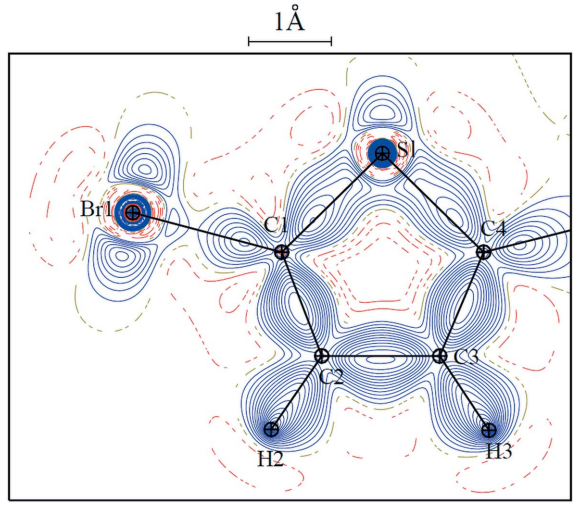

Figure 3
Deformation electron density transferred from the ELMAM2 database (contour: ±0.05 e Å^{-3}). In the electronic version of the paper, blue continuous line: positive; red dashed lines: negative; and yellow dashed lines: zero contours.

trostatically favourable interactions with O atoms when the C—*X*···O angle is not far from being flat. This characteristic charge-density distribution also has consequences in the stereochemistry of halogen–halogen interactions (Bui *et al.*, 2009). In the present structure, the Br atom also makes a weak interaction with H7*A* of another molecule at a distance of 3.002 Å; the H7*A*···Br1···O1 angle is 57.5°.

In addition, two different H···H interactions are found to contribute to the formation of the crystal packing. H2 makes a contact with H8*B* of an adjacent molecule at a distance of 2.316 Å (Fig. 2). H6*B* makes a comparatively shorter interaction with H6*B* of a neighbouring molecule at a distance of 2.079 Å through an inversion centre (Fig. 2). H···H interactions have been shown to have a stabilizing effect in molecules and crystals (Matta *et al.*, 2003).

To analyse quantitatively the intermolecular contacts in the title compound, a Hirshfeld surface analysis was performed with *CrystalExplorer* (Spackman & Jayatilaka, 2009). The analysis reveals that H···H (31.1%) and Br···H (25.1%) are the most prevalent interactions. The next major crystal packing interactions are S···H (14.4%), C···H (12.5%), O···H (10.3%) and Br···O (3.8%).

The thiophene and the dioxalane rings are planar and nonplanar, as expected, and the dihedral angle between the thiophene ring plane and the O2—C5—O1 plane in dioxalane is 55.1°. The two dioxolane rings adopt an *anti* conformation due to the intramolecular inversion centre. Viewed along the *c* axis, the molecules are stacked over each other and form two different sizes of channel. In the larger channel, two Br atoms of two neighbouring molecules point towards each other at a distance of 4.113 (4) Å.

When interatomic distances are compared between the spherical and the transferred models, most of the covalent bond lengths (between non-H atoms) are comparable within one or two times their standard uncertainties. The C5—O2 bond length shows the largest discrepancy as it decreases from 1.410 (2) to 1.406 (1) Å after transfer and subsequent structure refinement. The same trend is also observed for all other C—O bonds of the dioxolane group. This shortening of oxygen-containing covalent bonds can be explained by the fact that the modelling of oxygen electron lone pairs has an effect on the coordinates of the O atoms. When the spherical atom model (IAM) is used, the O atom is slightly displaced towards the middle of the lone pairs. The transfer procedure, followed by the refinement of the structural parameters, leads to removal of this bias on the O-atom coordinates, thus shortening the covalent bonds in which they are involved. This is confirmed by the values of the equivalent B_{iso} factor of O1 and O2, which also decrease slightly, upon transfer, by about 0.06 Å^2, which is above the standard uncertainty on B_{iso} parameters (∼0.02 Å^2). These observations clearly support the transfer of electron-density parameters as it gives a better structural model, unbiased by the nonmodelled deformation electron density.

In the comparison of the two structures, the H—*X* distances in the multipolar atom model are also elongated to the standard neutron diffraction values (Allen, 1986). These structural modifications have repercussions for some of the intermolecular contacts. For instance, the distance between the H6*B* atoms of two symmetry-related molecules is decreased significantly upon transfer from 2.275 to 2.079 Å.

There are two C8—H8*B*···O2 interactions in a dimer of molecules (Table 1) in the crystal structure which can be considered as a very weak hydrogen bond. These values are slightly different (2.67 Å and 142.0°) in the IAM structure. H8*B* also forms weak intramolecular contacts with atoms O1 and O2. In the H8*B*···O1 interaction, which generates a five-atom ring, the H···O distance is 2.69 Å but the C—H···O angle of 96.2° is unfavourable for a hydrogen bond. The corresponding values in the IAM model are 2.66 Å and 99.1°. The different positioning of the H atoms in the IAM model results in significantly altered geometric parameters of the hydrogen bonds, compared to the transferred models.

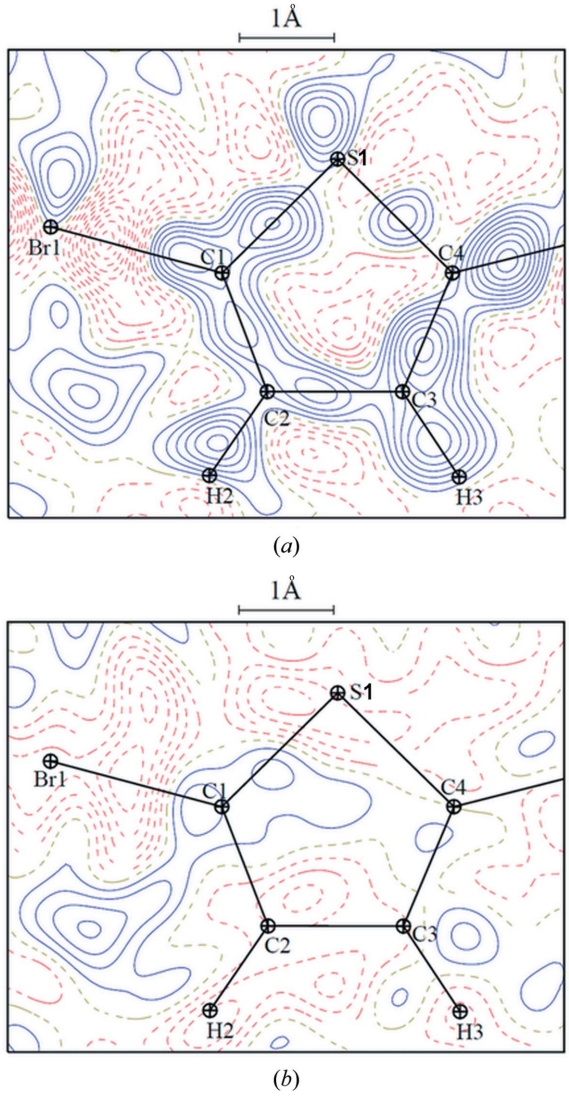

Figure 4
A Fourier map of residual density of the thiophene ring of the molecule shown (*a*) for the spherical atom model and (*b*) for the transferred multipolar atom model.

The transfer of the multipolar parameters significantly decreases the residual Fourier electron density. The maximum, minimum and r.m.s. values for the spherical atom model are 0.43, −0.68 and 0.090 e Å^{-3}, respectively. The corresponding values for the transferred–multipolar atom model are decreased to 0.33, −0.40 and 0.075 e Å^{-3}, respectively (Fig. 4). The electron-density parameters also allowed calculation of the dipole moment of the molecule (4.80 D; 1 D = 3.33564 $\times 10^{-30}$ C m).

Stevens & Coppens (1976) have introduced a suitability factor S for the multipolar atom model which is based on the observation that the improvement in the refinement statistics is mainly due to a better description of the valence electron density. The suitability factor S of a compound is equal to the following ratio: $S = V/(\Sigma n^2_{\rm core})$ where V is the unit-cell volume and $n_{\rm core}$ is the number of core electrons for the given atom types. The denominator is a measure of the core electron scattering of the unit cell. The suitability factor was calculated to be 0.235 for compound (I). This low value is due to the Br atom in the chemical formula. After the database transfer of compound (I), the difference $\Delta R(F)$ between the spherical atom model (0.027) and the transferred model (0.022) is 0.50. As illustrated by Dittrich *et al.* (2007), the lower the suitability factor, the lower is the expected $\Delta R(F)$.

A rigid bond test analysis shows that the r.m.s. difference of U_{ij} ellipsoids along the covalent bonds shows a slight improvement, with ΔZ = 0.0019 Å^2 for the IAM model and ΔZ = 0.0018 Å^2 for the transferred model. The magnitude of the displacement parameters also generally decreases upon the transfer: $U_{\rm eq}$(multipolar) ≈ $U_{\rm eq}$(IAM) × 0.96.

Experimental

For the synthesis of the title compound, the same procedure as that reported by Ellinger *et al.* (2007) was adopted, in toluene solvent (see Scheme in *Comment*). 1,4-Bis(5-bromothiophen-2-yl)butane-1,4-dione (1.0 g, 2.5 mmol) was dissolved in hot toluene (50 ml). After complete dissolution of the diketone, *p*-toluenesulfonic acid (*p*-TosH; 200 mg, 1.1 mmol) and ethylene glycol (10 ml, 179.3 mmol) were added. The mixture was then stirred and heated at 388 K for 48 h using a Dean–Stark trap. After cooling, saturated aqueous $NaHCO_3$ was added. The organic phase was separated and the aqueous phase was extracted with toluene three times. The combined organic phases were dried over anhydrous $MgSO_4$, filtered, evaporated to dryness and purified by fractional recrystallization using cyclohexane to give the title product (yield 48%). Crystals used for analysis were grown by slow evaporation from a chloroform solution at room temperature. ^{1}H NMR (200 MHz, $CDCl_3$): δ 6.9 (*d*, 2H, *J* = 3.8 Hz), 6.74 (*d*, 2H, *J* = 3.8 Hz), 3.98 (*m*, 8H, OCH_2CH_2O), 2.08 (*s*, 4H).

Crystal data

$C_{16}H_{16}Br_2O_4S_2$
M_r = 496.23
Monoclinic, *C*2/*c*
a = 19.2550 (10) Å
b = 5.7804 (4) Å
c = 16.9328 (6) Å
β = 112.845 (4)°
V = 1736.6 (3) Å^3
Z = 4
Mo *Kα* radiation
μ = 4.93 mm^{-1}
T = 100 K
0.37 × 0.20 × 0.20 mm

Table 1
Hydrogen-bond geometry (Å, °).

D—H···*A*	*D*—H	H···*A*	*D*···*A*	*D*—H···*A*
C8—H8*B*···O2^{i}	1.09	2.57	3.484 (1)	141

Symmetry code: (i) $-x+\frac{3}{2}, -y-\frac{1}{2}, -z+1$.

Data collection

Nonius KappaCCD diffractometer
Absorption correction: multi-scan (Blessing, 1995)
$T_{\rm min}$ = 0.329, $T_{\rm max}$ = 0.346
1565 measured reflections
1518 independent reflections
1478 reflections with $I > 2\sigma(I)$
$R_{\rm int}$ = 0.043

Refinement

$R[F^2 > 2\sigma(F^2)]$ = 0.021
$wR(F^2)$ = 0.053
S = 1.04
1518 reflections
109 parameters
H-atom parameters constrained
$\Delta\rho_{\rm max}$ = 0.33 e Å^{-3}
$\Delta\rho_{\rm min}$ = −0.40 e Å^{-3}

The space group was found to be *C*2/*c* and the reflections, including Friedel pairs, were merged with *SORTAV* (Blessing, 1987) before final refinement. Scale factors, atomic positions and displacement parameters were refined using *MoPro* software (Jelsch *et al.*, 2005) until convergence. The least-squares refinement was based on $|F|^2$.

Initially, a conventional spherical atom model was applied. Electron-density parameters were then transferred from the ELMAM2 library (Domagała *et al.*, 2011) for all the atoms, except C5, and were subsequently kept fixed. The C5 chemical atom type was not available in the ELMAM2 library and was modelled as atom C444 (c1-oCo-c2) in the UBDB theoretical database (Volkov *et al.*, 2004, 2007; Dominiak *et al.*, 2007). With the electron-density library transfer, the same structural parameters were refined but a multipolar charged atom model was applied. The molecule was set electrically neutral after library transfer. A view of the transferred deformation electron density is shown in Fig. 3.

The H—*X* distances were constrained to the standard values in the neutron diffraction studies (Allen, 1986): 1.092 Å for CH_2 and 1.083 Å for aromatic C—H groups. Riding constraints on H-atom isotropic displacement parameters were applied: $U_{\rm iso}$(H) = 1.2$U_{\rm eq}$(*X*), where *X* is the neighbouring C atom. The refinements were carried out using all reflections. The ELMAM2 refinement shows a slight improvement in the statistical indexes when compared to the spherical atom refinement. With a $I/\sigma_I > 2$ cutoff, the crystallographic factors are reduced from 0.0269 to 0.0212 for $R(F)$, and from 0.0409 to 0.0270 for $wR^2(F)$.

Data collection: *COLLECT* (Nonius, 2000); cell refinement: *SCALEPACK* (Otwinowski & Minor, 1997); data reduction: *DENZO* (Otwinowski & Minor, 1997); program(s) used to solve structure: *SIR92* (Altomare *et al.*, 1993); program(s) used to refine structure: *MoPro* (Jelsch *et al.*, 2005); molecular graphics: *Mercury* (Version 2.3;Macrae *et al.*, 2006) and *ORTEP-32* (Farrugia, 1997); software used to prepare material for publication: *pubCIF* (Westrip, 2010).

MA thanks the Higher Education Commission (HEC) of Pakistan for financial assistance. SN thanks the Islamia University of Bahawalpur Pakistan for financial assistance. We are very grateful to Emmanuel Wenger, CRM^2, for providing technical assistance.

Supplementary data for this paper are available from the IUCr electronic archives (Reference: KU3047). Services for accessing these data are described at the back of the journal.

References

Allen, F. H. (1986). *Acta Cryst.* B**42**, 515–522.
Altomare, A., Cascarano, G., Giacovazzo, C. & Guagliardi, A. (1993). *J. Appl. Cryst.* **26**, 343–350.
Auffinger, P., Hays, F. A., Westhof, E. & Ho, P. S. (2004). *Proc. Natl Acad. Sci. USA*, **101**, 16789–16794.
Blessing, R. H. (1987). *Crystallogr. Rev.* **1**, 3–58.
Blessing, R. H. (1995). *Acta Cryst.* A**51**, 33–38.
Brock, C. P., Dunitz, J. D. & Hirshfeld, F. L. (1991). *Acta Cryst.* B**47**, 789–797.
Bui, T. T. T., Dahaoui, S., Lecomte, C., Desiraju, G. R. & Espinosa, E. (2009). *Angew. Chem. Int. Ed.* **48**, 3838–3841.
Cao, Y., Bai, Y., Yu, Q., Cheng, Y., Liu, S., Shi, D., Gao, F. & Wang, P. (2009). *J. Phys. Chem. C*, **113**, 6290–6297.
Coppens, P. (1998). *Acta Cryst.* A**54**, 779–788.
Dittrich, B., Hübschle, C. B., Messerschmidt, M., Kalinowski, R., Girnt, D. & Luger, P. (2005). *Acta Cryst.* A**61**, 314–320.
Dittrich, B., Koritsánszky, T. & Luger, P. (2004). *Angew. Chem. Int. Ed.* **43**, 2718–2721.
Dittrich, B., Munshi, P. & Spackman, M. A. (2007). *Acta Cryst.* B**63**, 505–509.
Domagała, S. & Jelsch, C. (2008). *J. Appl. Cryst.* **41**, 1140–1149.
Domagała, S., Munshi, P., Ahmed, M., Guillot, B. & Jelsch, C. (2011). *Acta Cryst.* B**67**, 63–78.
Dominiak, P. M., Volkov, A., Li, X., Messerschmidt, M. & Coppens, P. (2007). *J. Chem. Theory Comput.* **3**, 232–247.
Ellinger, S., Ziener, U., Thewalt, U., Landfester, K. & Moller, M. (2007). *Chem. Mater.* **19**, 1070–1075.
Farrugia, L. J. (1997). *J. Appl. Cryst.* **30**, 565.
Gao, F., Wang, Y., Shi, D., Zhang, J., Wang, M., Jing, X., Humphry-Baker, R., Wang, P., Zakeeruddin, S. M. & Grätzel, M. (2008). *J. Am. Chem. Soc.* **130**, 10720–10728.
Guillot, B., Viry, L., Guillot, R., Lecomte, C. & Jelsch, C. (2001). *J. Appl. Cryst.* **34**, 214–223.
Hirshfeld, F. L. (1976). *Acta Cryst.* A**32**, 239–244.
Jelsch, C., Guillot, B., Lagoutte, A. & Lecomte, C. (2005). *J. Appl. Cryst.* **38**, 38–54.
Jelsch, C., Pichon-Pesme, V., Lecomte, C. & Aubry, A. (1998). *Acta Cryst.* D**54**, 1306–1318.
Kreyes, A., Amirkhani, M., Lieberwirth, I., Mauer, R., Laquai, F., Landfester, K. & Ziener, U. (2010). *Chem. Mater.* **22**, 6453–6458.
Kreyes, A., Ellinger, S., Landfester, K., Defaux, M., Ivanov, D. A., Elschner, A., Meyer-Friedrichsen, T. & Ziener, U. (2010). *Chem. Mater.* **22**, 2079–2092.
Li, Z. H., Wong, M. S., Fukutani, H. & Tao, Y. (2005). *Chem. Mater.* **17**, 5032–5040.
Ma, C.-Q., Fonrodona, M., Schikora, M. C., Wienk, M. M., Janssen, R. A. J. & Baüerle, P. (2008). *Adv. Funct. Mater.* **18**, 3323–3331.
Macrae, C. F., Edgington, P. R., McCabe, P., Pidcock, E., Shields, G. P., Taylor, R., Towler, M. & van de Streek, J. (2006). *J. Appl. Cryst.* **39**, 453–457.
Matta, C. F., Hernández-Trujillo, J., Tang, T. H. & Bader, F. W. (2003). *Chem. Eur. J.* **9**, 1940–1951.
Mazzeo, M., Pisignano, D., Favaretto, L., Barbarella, G., Cingolani, R. & Gigli, G. (2003). *Synth. Met.* **139**, 671–673.
Muzet, N., Guillot, B., Jelsch, C., Howard, E. & Lecomte, C. (2003). *Proc. Natl Acad. Sci. USA*, **100**, 8742–8747.
Nonius (2000). *COLLECT*. KappaCCD Linux Version. Nonius BV, Delft, The Netherlands.
Nyburg, S. C. & Faerman, C. H. (1985). *Acta Cryst.* B**41**, 274–279.
Otwinowski, Z. & Minor, W. (1997). *Methods in Enzymology*, Vol. 276, *Macromolecular Crystallography*, Part A, edited by C. W. Carter Jr & R. M. Sweet, pp. 307–326. New York: Academic Press.
Pichon-Pesme, V., Lecomte, C. & Lachekar, H. (1995). *J. Phys. Chem.* **99**, 6242–6250.
Roncali, J. (1992). *Chem. Rev.* **92**, 711–738.
Rousseau, T., Cravino, A., Ripaud, E., Leriche, P., Rihn, S., De Nicola, A., Ziessel, R. & Roncali, J. (2010). *Chem. Commun.* **46**, 5082–5084.
Ruysink, A. F. J. & Vos, A. (1974). *Acta Cryst.* A**30**, 503–506.
Spackman, M. A. & Jayatilaka, D. (2009). *CrystEngComm*, **11**, 19–32.
Stevens, E. D. & Coppens, P. (1976). *Acta Cryst.* A**32**, 915–917.
Volkov, A., Li, X., Koritsanszky, T. S. & Coppens, P. (2004). *J. Phys. Chem. A*, **108**, 4283–4300.
Volkov, A., Messerschmidt, M. & Coppens, P. (2007). *Acta Cryst.* D**63**, 160–170.
Westrip, S. P. (2010). *J. Appl. Cryst.* **43**, 920–925.
Zarychta, B., Pichon-Pesme, V., Guillot, B., Lecomte, C. & Jelsch, C. (2007). *Acta Cryst.* A**63**, 108–125.